

Quadruple bonding in C_2 and analogous eight-valence electron species

Sason Shaik^{1*}, David Danovich¹, Wei Wu², Peifeng Su², Henry S. Rzepa³ and Philippe C. Hiberty⁴

Triple bonding is conventionally considered to be the limit for multiply bonded main group elements, despite higher metal-metal bond orders being frequently observed for transition metals and lanthanides/actinides. Here, using high-level theoretical methods, we show that C_2 and its isoelectronic molecules CN^+ , BN and CB^- (each having eight valence electrons) are bound by a quadruple bond. The bonding comprises not only one σ - and two π -bonds, but also one weak 'inverted' bond, which can be characterized by the interaction of electrons in two outwardly pointing sp hybrid orbitals. A simple way of assessing the energy of the fourth bond is proposed and is found to be ~ 12 – 17 kcal mol⁻¹ for the isoelectronic species studied, and thus stronger than a hydrogen bond. In contrast, the analogues of C_2 that contain higher-row elements, such as Si_2 and Ge_2 , exhibit only double bonding.

The interest in multiple bonding has been on the rise ever since it was demonstrated that transition metals and lanthanides/actinides can form metal-metal bonding in which the maximum practical bond order reaches four to six bonds^{1–8}. In main elements, however, the maximum number of bonds between two atoms has remained three^{9–13}, this being composed of one σ - and two π -bonds. Nevertheless, there are diatomic molecules such as C_2 , Si_2 , CN^+ and BN , which, by having eight valence electrons, could at least formally express quadruple bonding between the two atoms (H. S. Rzepa, www.ch.imperial.ac.uk/rzepa/blog/?p=3065). One might then ask, no matter how naively, can the eight valence electrons (for example, between the two carbon atoms in C_2) couple to create four bonds and, if so, what is the bonding energy of the putative fourth bond? This is the focus of the present article, which uses valence bond (VB) theory^{12,14} and full configuration interaction (FCI) calculations to determine the bonding energy of the fourth bond in C_2 and its absence or presence in some of its isoelectronic species.

C_2 has been extensively investigated using a variety of methods, which have provided valuable information on its ground state ($X^1\Sigma_g^+$) and 17 of its excited states^{15–22}. Nevertheless, C_2 continues to challenge our understanding of bonding¹⁴. A nominal consideration of the bond order in the molecular orbital diagram in Fig. 1a would suggest a bond order of two²³, as in structure 1 in Fig. 1b, and, because the $2\sigma_g$ and $2\sigma_u$ orbitals are both filled, the molecule would then have two π -bonds unsupported by an underlying σ -bond (or a weak one assuming that $2\sigma_u$ is rather weakly antibonding), and two σ lone pairs. In contrast, using sp -hybridized carbons would suggest that it is possible to form a strong triple bond composed of one σ - and two π -bonds, with two electrons remaining in the outwardly pointing hybrids, as in structure 2 (Fig. 1b).

A recent VB theory study¹⁴ has shown that, by using structure 2, the properties of C_2 can be predicted quite well, and that its two electrons in the outwardly pointing hybrids are singlet-paired, thus yielding the known singlet ground state $X^1\Sigma_g^+$. The

directionality of these hybrids is the main factor that dictates why this 'inverted' fourth bond is commonly ruled out by chemists. However, a recent estimate of the bonding in [1.1.1]propellane²⁴ shows that such outwardly pointing hybrids may nevertheless maintain a highly significant bonding interaction. Indeed, if the two odd electrons in the outwardly pointing hybrids were very weakly coupled, the molecule would have exhibited a diradicaloid character with a closely lying triplet state. However, the diradicaloid character is absent²⁵. More compelling is the fact that the corresponding triplet state $c^3\Sigma_u^+$, in which these electrons are unpaired, lies 26.4 kcal mol⁻¹ above the ground state^{15,16}, indicating that these electrons maintain a significant bonding interaction in the ground state. Therefore, one cannot rule out the inference that C_2 has a quadruple bond, as depicted by structure 3 in Fig. 1b. Here, we test this hypothesis. We present an assessment of the energy of the fourth bond by means of VB and FCI calculations, and we demonstrate the quadruple bonding from the FCI wavefunction. As we shall show, although C_2 , CN^+ , BN and CB^- definitely have a fourth bond, higher-row analogues such as Si_2 or Ge_2 have only a double bond.

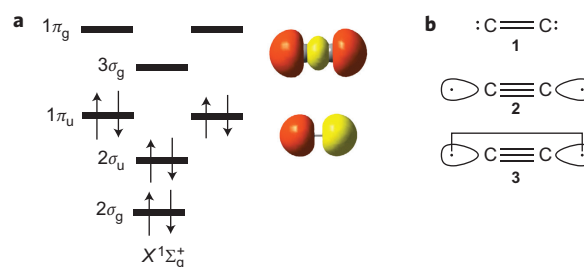


Figure 1 | Representations of bonding in C_2 . **a**, Molecular orbital diagram. The shapes of the $2\sigma_u$ and $3\sigma_g$ molecular orbitals, as determined from FCI calculations, are also represented together with their respective energy levels. **b**, Three simplified bonding cartoons.

¹Institute of Chemistry and The Lise Meitner-Minerva Center for Computational Quantum Chemistry, Hebrew University of Jerusalem, 91904, Jerusalem, Israel, ²The State Key Laboratory of Physical Chemistry of Solid Surfaces, Fujian Provincial Key Laboratory of Theoretical and Computational Chemistry, and College of Chemistry and Chemical Engineering, Xiamen University, Xiamen, Fujian 361005, China, ³Department of Chemistry, Imperial College London, South Kensington Campus, London SW7 2AZ, UK, ⁴Laboratoire de Chimie Physique, UMR CNRS 8000, Université de Paris Sud, 91405 Orsay Cédex, France. *e-mail: sason@yfaat.ch.huji.ac.il

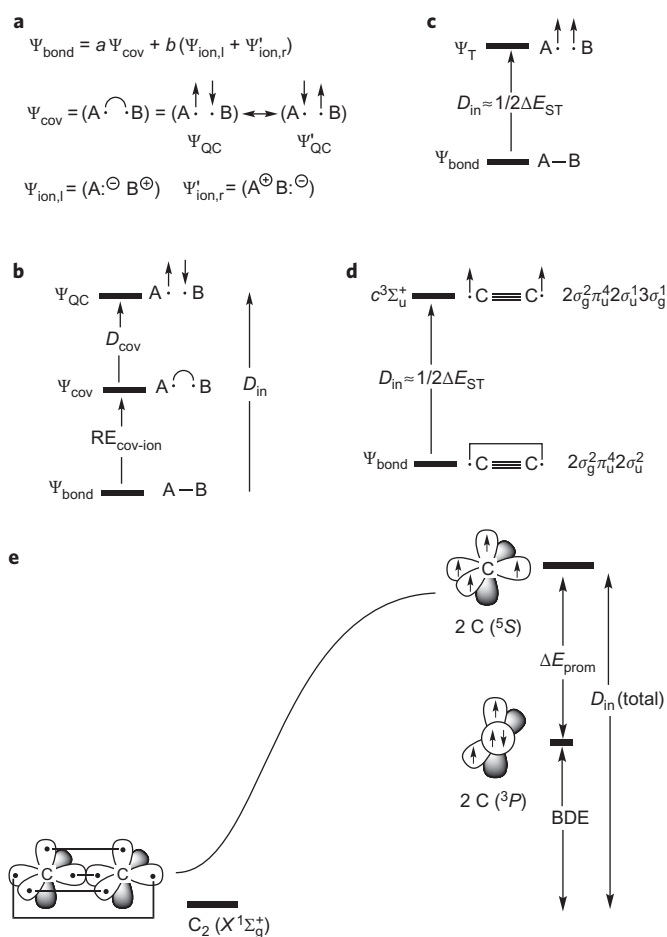


Figure 2 | VB wavefunctions and energy terms. **a**, The full-bond state (Ψ_{bond}) for bond A-B, with covalent (Ψ_{cov}) and two ionic (Ψ_{ion}) contributions, and the spin arrangement patterns that make up the covalent structure. **b**, Definition of the *in situ* bond energy (D_{in}) as the energy gap between Ψ_{bond} and the QC state Ψ_{QC} . $\text{RE}_{\text{cov-ion}}$ is the covalent-ionic resonance energy. **c**, Schematic energy diagram, showing D_{in} as half the energy gap (ΔE_{ST}) between the full bond state (Ψ_{bond}) and the triplet state (Ψ_{T}). **d**, Corresponding singlet $X^1\Sigma_g^+$ and triplet $c^3\Sigma_u^+$ C_2 states, needed for calculating D_{in} , and their dominant electronic configurations. **e**, Schematic representation of the dissociation of C_2 to two C atoms. $D_{\text{in}}(\text{total})$ is the intrinsic bonding energy due to bond-pairing of the prepared $\text{C}(^5\text{S})$ states, while the BDE measures the dissociation energy to the ground $\text{C}(^3\text{P})$ states. The promotion energy (ΔE_{prom}) is the $^3\text{P} \rightarrow ^5\text{S}$ difference (S and P are indicators of angular momentum).

Results and discussion

The fourth bond of C_2 . The bond dissociation energy (BDE) of one bond in a molecule like C_2 is meaningless. Hence, we calculate the *in situ* bond energy, D_{in} (refs 12,14,24,26), which measures the bonding interaction in a given bond. VB theory enables us to determine D_{in} for any bond using a reference non-bonding state, Ψ_{QC} , a so-called quasi-classical (QC) state^{12,14,24,26}, as illustrated in Fig. 2a,b. Thus, the wavefunction of the bond, Ψ_{bond} , is given in Fig. 2a as a combination of a covalent structure, Ψ_{cov} , and secondary ionic structures, Ψ_{ion} (refs 12,24,27). The covalent structure is stabilized by the resonance energy of its constituent spin-arrangement patterns, one with spin-up/spin-down and the other with spin-down/spin-up. Mixing of the ionic structures into the covalent structure further augments the bonding interaction with covalent-ionic resonance energy.

The QC state is one of the spin-arrangement patterns of Ψ_{cov} , and it is non-bonding as the two odd electrons in it maintain

only classical interactions, which sum to zero^{12,14,24,26}. In turn, D_{in} is the energy difference (Fig. 2b) of the Ψ_{QC} and of Ψ_{bond} states.

Figure 2c shows another way of estimating D_{in} by calculating the corresponding triplet state, Ψ_{T} , which uncouples the electrons of the fourth bond to a triplet state with two identical spins. As has been discussed previously²⁸ (see ref. 26, p. 131), the singlet-to-triplet excitation of a bond is approximately twice the desired D_{in} . Figure 2d shows the symbols for the C_2 states that are involved in this particular singlet-to-triplet excitation.

Figure 2e shows the relationship between the total D_{in} and BDE for all the electron pairs in C_2 . The BDE involves the relaxation of the fragments and their electronic demotion to the corresponding electronic ground states, which in the case of C atoms are the ^3P states. However, D_{in} (total) measures the stabilization energy due to bond-pairing of the ‘prepared’ ^5S states of C, without any effects associated with the relaxation of the fragments electronically (or geometrically if applicable). We shall refer to D_{in} (total) as the ‘intrinsic bonding energy’.

The first two entries in Table 1 list the D_{in} values for C_2 from VB theory. The two methods give values for D_{in} of the fourth C–C bond of 14.30 and 11.64 kcal mol⁻¹, respectively. We note that the VB-calculated ΔE_{ST} value (23.28 kcal mol⁻¹) is quite close to the experimental value of the vertical excitation from $X^1\Sigma_g^+$ to the $c^3\Sigma_u^+$ state (26.4 kcal mol⁻¹)^{15,16}. This is expected, because the VB calculation of ΔE_{ST} is entirely equivalent to the $X^1\Sigma_g^+ \rightarrow c^3\Sigma_u^+$ excitation that uncouples the singlet pair of the fourth-bond electrons to a triplet spin, as shown in Fig. 2c,d²⁹ (see also ref. 26, pp. 57,79,88,188).

Using molecular orbital-based FCI computations of ΔE_{ST} is a convenient alternative way to obtain D_{in} data. Indeed, our FCI calculations for these states in C_2 show that the ground-state $X^1\Sigma_g^+$ and the triplet-state $c^3\Sigma_u^+$ are dominated by the $2\sigma_g^2\pi_u^4 2\sigma_u^2$ and $2\sigma_g^2\pi_u^4 2\sigma_u^1 3\sigma_g^1$ configurations (Supplementary Section II.2). The calculated FCI value of ΔE_{ST} is 29.6 kcal mol⁻¹, slightly higher than the experimental value. Using the relation of D_{in} to ΔE_{ST} in Fig. 2c, we list the corresponding D_{in} values in Table 1 (last two entries), estimated from the experimental and FCI ΔE_{ST} quantities. These values are 13.2 and 14.8 kcal mol⁻¹. Thus, four different methods bracket the intrinsic bonding energy of the fourth bond in the range 11.6–14.8 kcal mol⁻¹.

To gauge the relative intrinsic bonding energy of this fourth C–C bond in relation to the others within the molecule, we used the same VB method and obtained 100.4 kcal mol⁻¹ for the internal $\sigma(\text{C}-\text{C})$ bond and 94.2 kcal mol⁻¹ for each of the two π -bonds, close to previously obtained values¹⁴. Thus, the fourth bond of C_2 has an intrinsic bonding energy value that is ~15% of the internal bonds in the molecule. Although this bond is not of great strength, it is nevertheless significant and cannot be ignored or dismissed.

Comparing the quadruple bond in C_2 to the triple bond in HCCH. Let us compare the intrinsic bonding energy of C_2 to that

Table 1 | Values of *in situ* bond energies (D_{in} , kcal mol⁻¹) for the fourth bond of diatomic molecules calculated in different ways.

Method	Source of D_{in}	C_2	BN	CN^+	CB^-
VBSCF/6-31G*	QC state	14.30	16.97	17.38	14.16
VBSCF/6-31G*	$\frac{1}{2}\Delta E_{\text{ST}}$	11.64	11.46	12.74	11.55
FCI/6-31G*	$\frac{1}{2}\Delta E_{\text{ST}}$	14.80	16.64	16.89	13.37
Experimental datum [†]	$\frac{1}{2}\Delta E_{\text{ST}}$	13.19 [†]	13.72 [‡]	-	-

[†]Ref. 15.

[‡]Ref. 46.

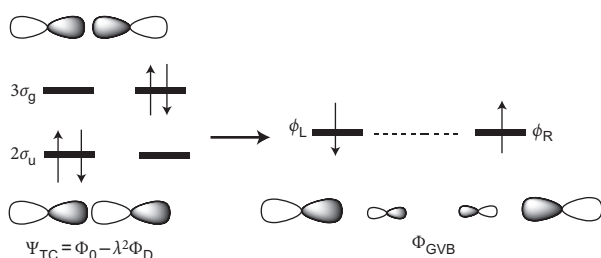


Figure 3 | Schematic representation of the transformation of the TC wavefunction (equation (3)) into a GVB wavefunction. The GVB orbitals are a λ -weighted sum and difference of the $2\sigma_u$ and $3\sigma_g$ molecular orbitals. The singlet coupling of the corresponding electrons is signified by the dotted line connecting the orbitals.

of HCCH (in which a triple bond binds the HC fragments) by reference to Fig. 2e. Summing up the calculated D_{in} values for the two π bonds, the σ bond and the fourth bond of C_2 , we obtain a total intrinsic bonding energy of $D_{in}(\text{total}) = 303 \text{ kcal mol}^{-1}$, which is the bonding interaction between the C atoms in their 5S states (see similar past analyses in refs 30–33). Thus, according to Fig. 2e, the $D_{in}(\text{total})$ value for C_2 is given by the sum of BDE and the corresponding promotion energies of the C fragments from the ground states (3P) to the high spin (5S) states, which are ‘prepared’ for bonding. Equation (1) expresses this relationship for any given molecule:

$$D_{in}(\text{total}) \approx \text{BDE} + \Delta E_{\text{prom}} \quad (1)$$

As FCI is too costly for HCCH, we used multi-reference configuration interaction (MRCI) calculations, which gave $D_{in}(\text{total}) = 313.7 \text{ kcal mol}^{-1}$ for C_2 , but only $252.7 \text{ kcal mol}^{-1}$ for HCCH. As such, computationally, the intrinsic bonding energy for C_2 is larger than for HCCH, in agreement with the relative bond multiplicities of 4 versus 3. Using experimental BDEs³⁴ (146.05 and $236.7 \text{ kcal mol}^{-1}$ for C_2 and HCCH, respectively) and promotion energies ($96.4 \text{ kcal mol}^{-1}$ per C atom³⁵ and $16.7 \text{ kcal mol}^{-1}$ $^2\Pi \rightarrow ^4\Sigma^-$ promotion energy per HC³⁴) gives $D_{in}(\text{total}) = 338.9 \text{ kcal mol}^{-1}$ for C_2 and $D_{in}(\text{total}) = 270.1 \text{ kcal mol}^{-1}$ for HCCH. These $D_{in}(\text{total})$ values lead again to the conclusion that the intrinsic bonding interaction in the quadruply bonded C_2 is larger than that in the triply bonded HCCH. Furthermore, because the $D_{in}(2\pi)$ values for C_2 and HCCH¹² are virtually identical (186 – $188 \text{ kcal mol}^{-1}$), this means that the intrinsic bonding energy of the internal σ_{CC} and inverted fourth bond of C_2 combined is significantly larger than the σ_{CC} bond of HCCH. This value can be further corrected by taking into account the ‘promotion’ term due to the different orbitals (rehybridization, size) of the high-spin fragments from their situation in the molecule relative to the free fragments. With this term, which is 11 kcal mol^{-1} larger for the two HC fragments than for the two C fragments, the resulting σ -bonding interaction in C_2 is 50 – 57 kcal mol^{-1} higher than for HCCH. This is a strong argument in support of the quadruple bond character of C_2 and its augmented bonding interaction compared with HCCH.

The $X^1\Sigma_g^+$ states of Si_2 and Ge_2 . Next we turned to the higher-row analogues of C_2 , Si_2 and Ge_2 . Using FCI, both were found to have two low-lying triplet ground states ($^3\Sigma_g^-$ and/or $^3\Pi_u$), in agreement with experiment for Si_2 and previous CI results^{36,37}. The singlet $X^1\Sigma_g^+$ states of Si_2 and Ge_2 lie significantly higher and are different to the corresponding state for C_2 (Supplementary Sections II.2.5 and II.2.6). Thus, in their singlet states, Si_2 and Ge_2 give up one of their π bonds, and instead populate the $(n+1)\sigma_g$ orbital (analogous to $3\sigma_g$ in Fig. 1a). Of the three filled σ orbitals, one is

weakly antibonding and two are bonding. As such, in their $^1\Sigma_g^+$ states, Si_2 and Ge_2 have double bonds composed of σ and π bonds, in line with the reluctance of higher-row molecules to form multiple π bonds^{38–41}.

Quadruple bonding in CN^+ , BN and CB^- . We next turned to the isoelectronic first-row analogues of C_2 with eight valence electrons: CN^+ , BN and CB^- (refs 42–47). For all cases we carried out FCI calculations to ascertain the nature of the ground or low-lying singlet states, and subsequently also calculated CN^+ , BN and CB^- by VB theory, using VBSCF/6-31G* (VBSCF refers to valence bond self-consistent field calculations; see Supplementary Sections II.2.2, II.2.3, II.2.4 for FCI and Tables S1–S5 for VBSCF).

It is well known that for C_2 and its isoelectronic first-row analogues the two lowest electronic states, $^3\Pi$ and $^1\Sigma^+$ types, are close in energy^{20,22,25,34,42–47}. This is what we indeed find, but the focus of our FCI and VB calculations is on the $^1\Sigma^+$ states, which are the only possible candidates to have quadruple bonding in the molecules at hand.

To ascertain the quadruple bonding in these three molecules we started with VB theory and followed with FCI. The VB results of the $^1\Sigma^+$ ground states for these molecules were analogous to those for C_2 . Table 1 shows that the D_{in} values for the fourth bond of these molecules can be bracketed in the range 11.6 – $17.4 \text{ kcal mol}^{-1}$. As already noted, this fourth bond, although weaker than the components of the internal triple bond, is significant and cannot be ignored.

C_2 bond orders and force constants. Interestingly, the double-hybrid density functional theory⁴⁸ calculated Wiberg bond order of C_2 is larger than 3 (it is 3.714 using the Kohn–Sham density). At the same level, the bond order of the C–C bond in HCCH is 2.998 , and in N_2 it is 3.032 (Supplementary Section III). These bond orders correlate with the above $D_{in}(\text{total})$ values we estimated for C_2 versus HCCH. In contrast, our relaxed force constant (RFC)⁴⁹ calculations show that HCCH has a larger RFC than C_2 (Supplementary Section IV). As one generally expects an increase in RFC with increasing bond multiplicity^{11,49}, this finding constitutes a puzzle; if indeed there is a fourth bond in singlet C_2 , then why does the triple bond in acetylene have a larger RFC than the quadruple bond in C_2 ? This is especially surprising, because the estimated total bonding energy relative to the ‘prepared’ fragments (*vide supra*) for C_2 is larger than the analogous quantity for acetylene. The fact that the relative bonding energies are not reflected in the RFCs indicates the existence of factors that soften the potential energy of C_2 near the minimum. A plausible explanation for such a curve-flattening factor is the avoided crossing that occurs between the $B^1\Sigma_g^+$ state and the $X^1\Sigma_g^+$ ground state²¹ at a distance (1.6 \AA) quite close to the equilibrium distance. Furthermore, the $B^1\Sigma_g^+$ state is dominated by

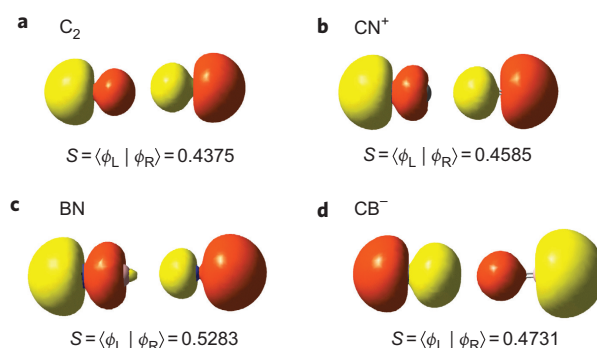


Figure 4 | Semi-localized ϕ_L - ϕ_R orbitals, which form the fourth bond and their overlap S values. a, C_2 . b, CN^+ . c, BN . d, CB^- .

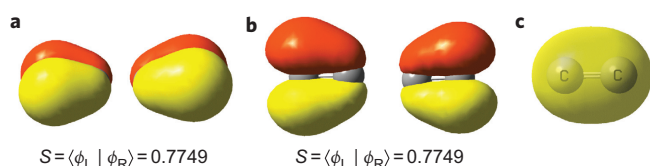


Figure 5 | ϕ_L - ϕ_R GVB orbital pairs and their overlap S values for the internal bonds in C_2 . **a-c**, π out-of-plane (**a**), π in-plane (**b**) and internal σ bond (**c**) represented by the $2\sigma_g$ molecular orbital.

configurations that display one less π bond than the $X^1\Sigma_g^+$ ground state. These factors can flatten the ground state near the equilibrium geometry but will not affect the well depth, and as such will lower the RFC of C_2 relative to acetylene, despite the quadruple bonding in the former.

Nature of the fourth bond in C_2 , CN^+ , BN and CB^- revealed by full CI. The fourth bond can be easily understood using VB language as a hybrid of covalent and ionic structures (Fig. 2a), similarly to any other bond^{14,27}. Although the VB mechanism is straightforward, one may wonder what FCI tells us about the nature of the fourth bond?

Inspection of the FCI results for the four molecules that exhibit quadruple bonding reveals that, in all of them, the FCI wavefunction is dominated by a mixture of the fundamental configuration, Φ_0 , and a smaller and negatively signed contribution from the doubly excited one, Φ_D (in which two electrons that populate the weakly antibonding σ orbital in Φ_0 now populate the previously vacant bonding σ orbital in Φ_D). For C_2 , these are the $2\sigma_u$ and $3\sigma_g$ orbitals depicted in Fig. 1a, whereas for heteronuclear diatomics such as CN^+ , these are 4σ and 5σ , which are the analogous weakly antibonding and weakly bonding orbitals, respectively. These two configurations constitute $\sim 80\%$ of the total weight of the FCI wavefunction. The rest of the configurations have much smaller weights and we shall deal with their significance later. Therefore, to a first approximation, the FCI wavefunction can be written in terms of the two leading configurations with corresponding coefficients C_0 and C_D . For example, for C_2 we have the following wavefunction where Φ_0 and Φ_D are expressed in their Slater-determinant representations:

$$\Psi_{\text{FCI}} = C_0 \left| (2\sigma_g^2 1\pi_u^2 1\pi_u^2) 2\sigma_u \bar{2}\sigma_u \right| - C_D \left| (2\sigma_g^2 1\pi_u^2 1\pi_u^2) 3\sigma_g \bar{3}\sigma_g \right| + \dots \quad (2)$$

where $C_0 = 0.828$, $C_D = 0.324$. Here, the orbital terms in parentheses correspond to the closed-shell part of the two configurations, consisting of the filled $2\sigma_g$ and doubly degenerate $1\pi_u$ orbitals (Fig. 1), written schematically. On the other hand, the part that undergoes a change from Φ_0 to Φ_D is written explicitly, with the bar over the orbital indicating spin β , and the lack of bar indicating spin α .

Taking now the leading two configurations (TC) and dropping the normalization constant, we obtain the following wavefunction:

$$\Psi_{\text{TC}} = \left| (2\sigma_g^2 1\pi_u^2 1\pi_u^2) 2\sigma_u \bar{2}\sigma_u \right| - \lambda^2 \left| (2\sigma_g^2 1\pi_u^2 1\pi_u^2) 3\sigma_g \bar{3}\sigma_g \right| \quad (3)$$

where $\lambda^2 = C_D/C_0 = 0.6255$. As in the textbook example of the TC wavefunction for H_2 (ref. 26, pp. 42 and 241, and refs 50,51) the Ψ_{TC} in equation (3) can also be transformed to a generalized valence bond (GVB) wavefunction (Supplementary Sections II.3), with two singly occupied orbitals that are spin-paired to a bond, as illustrated in Fig. 3. Thus, combining and subtracting the $2\sigma_u$ and $3\sigma_g$ orbitals, the TC wavefunction remains invariant, and we have two semi-localized orbitals. The so-called ϕ_L is localized at the

left-hand carbon atom, with a smaller tail on the right-hand carbon, whereas the other, ϕ_R , is localized on the right-hand carbon and has a tail on the left-hand atom^{50,51}. The electrons in the ϕ_L and ϕ_R orbitals are singlet-paired, which in Fig. 3 is symbolized by the dotted line connecting the two singly occupied orbitals.

The two transformed orbitals for all the molecules are shown in Fig. 4 together with S , a measure of their overlap. The larger the overlap in the GVB pairs⁵¹, the stronger the respective bond. The significant overlaps in Fig. 4 underscore the conclusion that the bond energies of the fourth bond are significant in all these cases.

In fact, it is easily seen that the Ψ_{TC} wavefunction describes a quadruple bond. Merely reading equation (2) reveals that the C_2 molecule has an internal triple bond, composed of three strongly bonding orbitals populated by six electrons, $2\sigma_g^2 1\pi_u^4$ and a fourth bond made from the transformed ϕ_L - ϕ_R GVB pair. The same picture is true for the other molecules; they all have an internal triple bond made from the $2\sigma^2 1\pi^4$ sub-shell, which is augmented by a GVB pair ϕ_L - ϕ_R . By common knowledge (ref. 26, pp. 42 and 241, refs 50,51) the GVB wavefunction of a pair like ϕ_L - ϕ_R is equivalent to the localized VB picture in Fig. 2a.

In fact, the FCI wavefunction describes all the other bonds in the same manner (Supplementary Sections II.3.2 and II.3.3). Thus, in addition to Φ_D , which correlates the electrons of the fourth bond, there are also two negatively signed configurations, which correlate the electrons in the two internal π bonds, for example $|2\sigma_g^2 2\sigma_u^2 1\pi_{ux}^2 1\pi_{gy}^2\rangle$ and $|2\sigma_g^2 2\sigma_u^2 1\pi_{uy}^2 1\pi_{gx}^2\rangle$, which can be combined with the fundamental configuration, as in equation (3), to generate a TC wavefunction with two π -GVB pairs. The only bond that is not correlated in this manner by the FCI wavefunction is the internal σ (C-C) bond, which is rather well described by the doubly occupied $2\sigma_g$ orbital, and its corresponding di-excited configuration is too high to mix appreciably into the CI wavefunction. Figure 5a,b depicts the ϕ_L - ϕ_R GVB pairs for the in-plane and out-of-plane π bonds, and Fig. 5c shows the internal σ_{CC} bond represented by the $2\sigma_g$ orbital. As such, together with the ϕ_L - ϕ_R pair of the fourth bond (Fig. 4a), we have a quadruple bond in C_2 .

The same applies to all four first-row molecules studied here (Supplementary Sections II.3.4–II.3.6). Thus, because GVB bond pairs are by definition mixtures of covalent and ionic structures (Fig. 2a)^{50,51}, the FCI and VB descriptions of C_2 , CN^+ , BN and CB^- are in fact completely equivalent; both pictures view these molecules as quadruply bonded species. The fourth bond is thus established herein by two independent and high-level computational procedures. Quadruple bonding is indeed possible in first-row main-group elements (H. S. Rzepa, www.ch.imperial.ac.uk/rzepa/blog/?p=3065).

Conclusions

We have shown herein, by a combination of FCI and VB calculations, that the ground or low-lying $^1\Sigma^+$ singlet states of the molecules C_2 , CN^+ , BN and CB^- are all quadruply bonded, having three internal bonds (one σ and two π) and one weak 'inverted' C-C bond. The intrinsic bonding energy of the fourth bond is bracketed in the range 12–17 kcal mol⁻¹, which is much stronger than a hydrogen bond, and is certainly stronger than the δ and ϕ bonds in dimers of transition metals and lanthanides/actinides. As such, it is a bond, as depicted in 3 in Fig. 1b. Thus, our study shows that quadruple bonding also exists in main group element chemistry. Other species that are likely to exhibit quadruple bonding include, for example, N_2^{2+} , NO^{3+} and BO^+ .

One may wonder what might be the experimental manifestations of the fourth bond? A lack of radical reactivity relative to genuine radical or diradical species is perhaps one feature, but there may

be others. Here, in articulating such a fundamental feature of chemical bonding, we hope to promote the search for other experimental manifestations.

Note added in proof: The authors became aware of a further relevant paper that they would like to cite: Schleyer, P. v. R., Maslak, P., Chandrasekhar, J. & Grev, R. Is a CC quadruple bond possible? *Tetrahedron Lett.* **34**, 6387–6390 (1993).

Methods

The $^1\Sigma^+$ and $^3\Sigma^+$ states ($X^1\Sigma_g^+$ and $c^3\Sigma_u^+$ for homonuclear diatomics) of all the molecules (C_2 , Si_2 , Ge_2 , CN^+ , BN and CB^-) were calculated at the FCI/6-31G* level using the package MOLPRO-2010.1 (ref. 52). The FCI procedure excluded the core electrons and included $\sim 2 \times 10^8$ determinants. Force constants (f , in $N\text{ cm}^{-1}$) for both singlet C_2 and HCCH were calculated using the equation

$$f = 4\pi^2 c^2 \bar{\nu}^2 \mu \quad \mu = \frac{m_1 \cdot m_2}{m_1 + m_2}$$

where the frequency values $\bar{\nu}$ (in cm^{-1}) were obtained with MOLPRO using MRCI/6-31G*. RFC values were calculated using the Compliance program⁵³ using as an input the results from the Gaussian-03 CCSD(T)/6-31G* calculations (where CCSD(T) is 'coupled cluster including singles and double with perturbative triples'). MRCI/6-31G* calculations of the intrinsic bonding energy were carried out using CASSCF reference configurations (CASSCF is the 'complete active space self-consistent field'). For C_2 it was found that using two leading configurations in the FCI wavefunction as a basis for MRCI leads to results on a par with FCI.

The VB calculations were carried out for C_2 , CN^+ , BN and CB^- at the VBSCF/6-31G* level¹⁴ using the XMVB package⁵⁴. The VB structure set includes, as before, 92 structures, of which 21 involve four electron pairs that all make bonds between the atoms (Supplementary Sections I and Scheme S.1). The VBSCF/6-31G* calculations for each species involved the QC reference state as well as the $^1\Sigma^+(X^1\Sigma_g^+)$ and $^3\Sigma^+(c^3\Sigma_u^+)$ states, all carried out at the FCI/6-31G* optimized bond lengths for the corresponding singlet states (see Supplementary Information).

Received 25 October 2011; accepted 20 December 2011;
published online 29 January 2012

References

- Cotton, F. A. Metal–metal bonding in $[Re_2X_8]^{2-}$ ions and other metal atom clusters. *Inorg. Chem.* **4**, 334–336 (1965).
- McGrady, J. E. Electronic structure of metal–metal bonds, in *Computational Inorganic and Bioinorganic Chemistry* (eds Solomon, E. I., Scott, R. A. & King, R. B.) 425–431 (Wiley, 2009).
- Frenking, G. Building a quintuple bond. *Science* **310**, 796–797 (2005).
- Gagliardi, L. & Roos, B. O. Quantum chemical calculations show that the uranium molecule U_2 has a quintuple bond. *Nature* **433**, 848–851 (2005).
- Landis, C. R. & Weinhold, F. Origin of trans-bent geometries in maximally bonded transition metal and main group molecules. *J. Am. Chem. Soc.* **128**, 7335–7345 (2006).
- Xu, B., Li, Q.-S., Xie, Y., King, B. B. & Schaefer III, H. F. Metal–metal quintuple and sextuple bonding in bent dimetallocenes of the third row transition metals. *J. Chem. Theor. Comput.* **6**, 735–746 (2010).
- Tsai, Y.-C. & Chang, C.-C. Recent progress in the chemistry of quintuple bonds. *Chem. Lett.* **38**, 1122–1129 (2009).
- Takagi, N., Krapp, A. & Frenking, G. Bonding analysis of metal–metal multiple bonds in $R_3M-M'R_3$ ($M, M' = Cr, Mo, W$; $R = Cl, NMe_2$). *Inorg. Chem.* **50**, 819–826 (2011).
- Fischer, R. C. & Power, P. P. π -Bonding and the lone pair effect in multiple bonds involving heavier main group elements: developments in the new millennium. *Chem. Rev.* **110**, 3877–3923 (2010).
- Kravchenko, V. *et al.* Solid-state ^{29}Si NMR study of $RSiSiR$: a tool for analyzing the nature of the Si–Si bond. *J. Am. Chem. Soc.* **128**, 14472–14473 (2006).
- Schreiner, P., Reisenauer, H. P., Romanskii, J. & Mloston, G. A formal carbon–sulfur triple bond: $H-C\equiv S-O-H$. *Angew. Chem. Int. Ed.* **48**, 8133–8136 (2009).
- Ploshnik, E., Danovich, D., Hiberty, P. C. & Shaik, S. The nature of the idealized triple bonds between principal elements and the σ origins of trans-bent geometries—a valence bond study. *J. Chem. Theor. Comput.* **7**, 955–968 (2011).
- Pease, R. N. An analysis of molecular volumes from the point of view of the Lewis–Langmuir theory of molecular structure. *J. Am. Chem. Soc.* **43**, 991–1004 (1921).
- Su, P., Wu, J., Gu, J., Wu, W., Shaik, S. & Hiberty, P. C. Bonding conundrums in the C_2 molecule: a valence bond study. *J. Chem. Theor. Comput.* **7**, 121–130 (2011).
- Weltner, W. Jr & van Zee, R. J. Carbon molecules, ions, and clusters. *Chem. Rev.* **89**, 1713–1747 (1989).
- Boggio-Pasqua, M., Voronin, A. I., Halvick, P. & Rayez, J.-C. Analytical representations of high level *ab initio* potential energy curves of the C_2 molecule. *J. Mol. Struct.* **531**, 159–167 (2000).
- Abrams, M. L. & Sherrill, C. D. Full configuration interaction potential energy curves for the $X^1\Sigma_g^+$, $B^1\Delta_g$, and $B^1\Sigma_g^+$ states of C_2 : a challenge for approximate methods. *J. Chem. Phys.* **121**, 9211–9219 (2004).
- Sherrill, C. D. & Piecuch, P. The $X^1\Sigma_g^+$, $B^1\Delta_g$, and $B^1\Sigma_g^+$ states of C_2 : a comparison of renormalized coupled-cluster and multireference methods with full configuration interaction benchmarks. *J. Chem. Phys.* **122**, 124104 (2005).
- Pradhan, A. D., Partridge, H. & Bauschlicher, C. W. Jr. The dissociation energy of CN and C_2 . *J. Chem. Phys.* **101**, 3857–3861 (1994).
- Peterson, K. A. Accurate multireference configuration interaction calculations on the lowest $^1\Sigma^+$ and $^3\Pi$ electronic states of C_2 , CN^+ , BN , and BO^+ . *J. Chem. Phys.* **102**, 262–277 (1995).
- Varandas, A. J. C. Extrapolation to the complete-basis-set limit and the implications of the avoided crossings: the $X^1\Sigma_g^+$, $B^1\Delta_g$, and $B^1\Sigma_g^+$ states of C_2 . *J. Chem. Phys.* **129**, 234103 (2008).
- Leininger, M. L., Sherrill, C. D., Allen, W. D. & Schaefer, III H. F. Benchmark configuration interaction spectroscopic constants for $X^1\Sigma_g^+ C_2$ and $X^1\Sigma^+ CN^+$. *J. Chem. Phys.* **108**, 6717–6721 (1998).
- Levine, I. N. *Quantum Chemistry*, 2nd edn, 321, table 13.2 (Allyn and Bacon, 1974).
- Wu, W., Gu, J., Song, J., Shaik, S. & Hiberty, P. C. The 'inverted' bond in [1.1.1] propellane is a charge-shift bond. *Angew. Chem. Int. Ed.* **48**, 1407–1410 (2009).
- Leininger, M. L., Allen, W. D., Schaefer, III H. F. & Sherrill, C. D. Is Møller–Plesset perturbation theory a convergent *ab initio* method? *J. Chem. Phys.* **112**, 9213–9222 (2000).
- Shaik, S. S. & Hiberty, P. C. *A Chemist's Guide to Valence Bond Theory*, 49–51 (John-Wiley & Sons, 2008).
- Shaik, S., Danovich, D., Wu, W. & Hiberty, P. C. Charge-shift bonding and its manifestations in chemistry. *Nature Chem.* **1**, 443–449 (2009).
- Shaik, S. S. A qualitative valence bond approach to organic reactions, in *New Theoretical Concepts for Understanding Organic Reactions* (eds Bertran, J. & Ciszmadia, G. I.) NATO ASI Series C267 (Kluwer Publishers, 1989).
- Shaik, S. Valence bond all the way: from the degenerate hydrogen exchange to cytochrome P450. *Phys. Chem. Chem. Phys.* **12**, 8706–8720 (2010).
- Lein, M., Krapp, A. & Frenking, G. Why do heavy-atom analogs of acetylene E_2H_2 ($E = Si-Pb$) exhibit unusual structures? *J. Am. Chem. Soc.* **127**, 6290–6299 (2005).
- Trinquier, G. & Malrieu, J. P. Nonclassical distortions at multiple bonds. *J. Am. Chem. Soc.* **109**, 5303–5315 (1987).
- Carter, E. A. & Goddard, W. A. Relation between singlet–triplet gaps and bond energies. *J. Phys. Chem.* **90**, 998–1001 (1986).
- Sugiyama, Y. *et al.* Synthesis and properties of a new kinetically stabilized digermene: new insights for a germanium analogue of an alkyne. *J. Am. Chem. Soc.* **128**, 1023–1031 (2006).
- Huber, P. K. & Herzberg, G. *Molecular Spectra and Molecular Structure IV. Constants of Diatomic Molecules* (Van-Nostrand-Reinhold, 1979).
- Moore, C. E. *Atomic Energy Levels, Vol. I (Hydrogen through Vanadium)*, Circular of the National Bureau of Standards 467 (US Government Printing Office, 1949).
- Ojha, K. S. & Gopal, R. Laser produced spectrum of Si_2 molecule in the region of 540–1010 nm. *Spectrochimica Acta Part A* **71**, 1003–1006 (2008).
- Bauschlicher, C. W. Jr & Langhoff, S. R. *Ab initio* calculations on C_2 , Si_2 , and SiC . *J. Chem. Phys.* **87**, 2919–2924 (1987).
- Karni, M. *et al.* HCSiF and HCSiCl: the first detection of molecules with formal $C\equiv Si$ triple bonds. *Angew. Chem. Int. Ed.* **38**, 332–335 (1999).
- Kutzelnigg, W. Chemical bonding in higher main group elements. *Angew. Chem. Int. Ed. Engl.* **23**, 272–295 (1984).
- Frenking, G. & von Hopffgarten, M. Calculation of bonding properties, in *Computational Bioinorganic and Inorganic Chemistry* (eds Solomon, E. I., Scott, R. A. & King, R. B.) 3–15 (John Wiley & Sons, 2009).
- West, R. Chemistry of the silicon–silicon double bond. *Angew. Chem. Int. Ed. Engl.* **26**, 1201–1211 (1987).
- Müller, T., Dallos, M., Lischka, H., Dubrovay, Z. & Szalay, P. G. A systematic theoretical investigation of the valence excited states of the diatomic molecules B_2 , C_2 , N_2 and O_2 . *Theor. Chem. Acc.* **105**, 227–243 (2001).
- Karton, A. & Martin, J. M. L. The lowest singlet–triplet excitation energy of BN : a converged coupled cluster perspective. *J. Chem. Phys.* **125**, 144313 (2006).
- Oncak, M. & Srncak, M. Electronic structure and physical properties of M_iX_i clusters ($M = B, Al$; $X = N, P$; $i = 1, 2, 3$): *ab initio* study. *J. Comput. Chem.* **29**, 233–246 (2008).
- Li, X. Z. & Pedale, J. Singlet–triplet separation in BN and C_2 : simple yet exceptional systems for advanced correlated methods. *Chem. Phys. Lett.* **431**, 179–184 (2006).
- Asmis, K. R., Taylor, T. R. & Neumark, D. M. Anion photoelectron spectroscopy of BN^- . *Chem. Phys. Lett.* **295**, 75–81 (1998).

47. Tzeli, D. & Mavridis, A. First-principles investigation of the boron and aluminum carbides BC and AlC and their anions BC^- and AlC^- . 1. *J. Phys. Chem. A* **105**, 1175–1184 (2001).
48. Grimme, S. Semiempirical hybrid density functional with perturbative second-order correlation. *J. Chem. Phys.* **124**, 034108 (2006).
49. Brandhorst, K. & Grunenberg, J. How strong is it? The interpretation of force and compliance constants as bond strength descriptors. *Chem. Soc. Rev.* **37**, 1558–1567 (2008).
50. Coulson, C. A. & Fischer, I. Notes on the molecular orbital treatment of the hydrogen molecule. *Phil. Mag. Series 7* **40**, 386–393 (1949).
51. Goddard III, W. A. & Harding, L. B. The description of chemical bonding from *ab initio* calculations. *Annu. Rev. Phys. Chem.* **29**, 363–396 (1978).
52. Werner, H.-J. *et al.* MOLPRO, version 2010.1 (University College Cardiff Consultants Limited, UK).
53. Brandhorst, K. & Grunenberg, J. Efficient computation of compliance matrices in redundant internal coordinates from cartesian Hessians for nonstationary points. *J. Chem. Phys.* **132**, 184101 (2010).
54. Song, L., Wu, W., Mo, Y. & Zhang, Q. *XMVB: an ab initio non-orthogonal valence bond program* (Xiamen University, China, 2003).

Author contributions

S.S. designed the project, analysed the FCI wavefunctions and wrote the paper. D.D. performed the VB, MRCI, FCI and bond order calculations. W.W. designed the initial VB calculations of C_2 . P.S. performed the initial set of VB calculations for C_2 . P.C.H. participated in the design of the VB determination of D_m , in the analysis of the FCI wavefunctions, and contributed to writing the manuscript. H.R. initiated interest in the problem¹⁴, and explored probes for characterizing the bonding properties.

Additional information

The authors declare no competing financial interests. Supplementary information accompanies this paper at www.nature.com/naturechemistry. Reprints and permission information is available online at <http://www.nature.com/reprints>. Correspondence and requests for materials should be addressed to S.S.